

Estimating Pedestrian Flow in Crowded Situations with Data Assimilation

Shusuke Shigenaka¹, Shunki Takami^{1,2}, Masaki Onishi¹,
Tomohisa Yamashita³, and Itsuki Noda¹

¹ National Institute of Advanced Industrial Science and Technology, Japan
{shusuke-shigenaka,s-takami,onishi-masaki,i.noda}@aist.go.jp

² University of Tsukuba, Japan

³ Hokkaido University, Japan
tomohisa@complex.ist.hokudai.ac.jp

Abstract. Recently, data assimilation (DA) has been used to examine large-scale phenomena such as global warming and ocean characteristics. It involves integrating real-world measurement data into a numerical model to increase the reproducibility of a simulation. This study aims to use DA to reproduce the movement of pedestrians in a crowded situation. Simulation experiments are performed using multi-agent simulation and parameters search to estimate the motion of large pedestrians is performed using genetic algorithm (GA). We compared the accuracy of the result obtained by simulation using the data of the number of people acquired via camera and the data of movement information acquired by Global Positioning System (GPS). When evaluating the simulation results, the accuracy is defined using the Nash–Sutcliffe model efficiency coefficient. Three GA methods are implemented to estimate the parameters and are evaluated using actual data from a Kanmon Strait Fireworks Display. The data assimilation method of this study was able to reproduce the real space with approximately 80% accuracy using the Nash–Sutcliffe model efficiency coefficient.

Keywords: Pedestrian Tracking · Pedestrian Simulation · Data Assimilation.

1 Introduction

Several studies are being conducted to measure and simulate the flows of pedestrians in crowded environments, such as the Olympics and festivals, with an aim to alleviate congestion and guide people to safety during disasters. In these studies, demonstration experiments on the scale of hundreds of people have been conducted in a public facility. Moreover, in a recent demonstration experiment, large-scale measurements and simulations of a Kanmon Strait Fireworks Display (**Fig. 1**) were conducted with several 10,000–100,000 people. However, in studies regarding large-scale targets on a global scale, it is difficult to observe every person in every area. Therefore, we propose the data assimilation (DA) method to estimate the flow of all the pedestrians in all the areas.

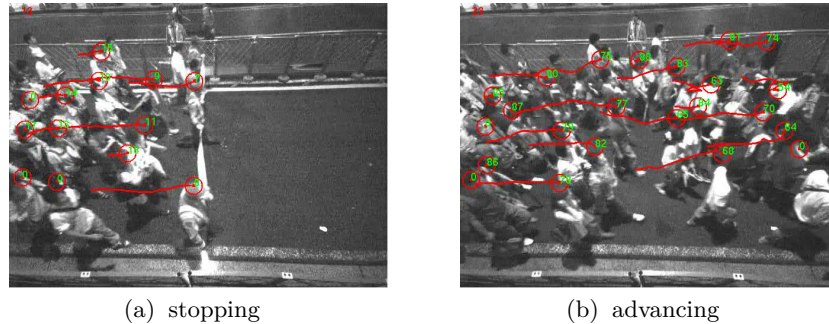


Fig. 1. Measurement of pedestrian at a Kanmon Strait Fireworks Display.

DA method modifies simulation results by applying actual observational data to simulation models and parameters. It is used to estimate large-scale phenomena such as global warming and ocean characteristics. Recently, large-scale measurement experiments of pedestrian flows have been performed. Using DA to analyze large-scale pedestrian flows is expected to increase the reproducibility of simulations.

Measurement experiments are being conducted, which involve a Kanmon Strait Fireworks Display held on August 13 every year since 2012 on the Kanmon Strait between Shimonoseki and Kita Kyushu City in Japan. We have studied various measures to alleviate congestion using the pedestrian simulator CrowdWalk [1] that simulates the flow of pedestrians at the Kanmon Strait Fireworks Display. To avoid crowd accidents, the executive committee of the Kanmon Strait Fireworks Display controls the movement of pedestrians by stopping and advancing them, as shown in **Fig. 1**; **Fig. 2** shows 10 control positions. However, to guide the crowd safely, the flow of all pedestrians at the measurement in actual environment and the entire venue of the Kanmon Strait Fireworks Display must be known.

Herein, a DA method is proposed for estimating the flow of pedestrians throughout the venue, including areas that are not covered by video cameras. This method incorporates the flow data collected from the Kanmon Strait Fireworks Display into the simulation, thereby increasing the reproducibility of the control information supplied to the executive committee.

2 Related studies

Notably, research of pedestrian measurement using multi-agent simulation is mainstream.

Galea et al. [2] proved that blended wing body (BWB) aircraft bearing around 1000 passengers and crew could provide evacuation as per safety standards using airEXODUS aircraft evacuation model [3] and fire simulation SMART-FIRE [4]. Tang et al. [5] proved that the Agent-based simulation can predict certain “bottleneck” areas with potential congestion except during panic (e.g.,



Fig. 2. Map showing the layout of the Kanmon Strait Fireworks Display, including the control positions.

accident site). However, such research pertains only indoor scenarios and only few research has been conducted regarding large-scale measurements to date.

DA has been used to improve the reproducibility of social phenomena estimated on a large scale. DA is primarily studied using the Kalman filter [6], the particle filter [7], and the four-dimensional variational method [8]. Miyoshi proposed “big data assimilation” to deal with the enormous amount of data using phased array weather radar and supercomputer “K”. Big data assimilation succeeded in reproducing the movement of guerilla heavy rain and a sudden local heavy downpour, with resolutions from 1 [km] to 100 [m] [9].

Recently, improvements in measurement technology allow the measurement of large-scale flows of people. Therefore, this study proposes a method for estimating the flow of 10,000–100,000 of people from partial measurement data using DA.

3 Overview of data assimilation

The proposed DA method is outlined herein using **Fig. 3**.

Step 1 Measurement of rough observation data

Image recognition applied to the camera pictures was used to measure the number of people moving into the Mojiko Station from 19:00 to 24:00 on the event day of the Kanmon Strait Fireworks Display. Global Positioning System (GPS) information about selected individuals moving from the event location to the Mojiko Station was measured after every 15 [min] for three different return paths along with the time required to reach the Mojiko Station for each path. These data pertain to only a certain area and certain individuals; thus, they are referred as rough observational data. The measurement methods are explained in **Sections 4.1** and **4.2**.

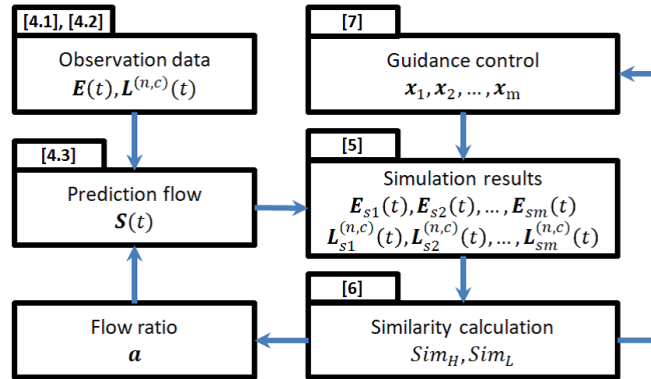


Fig. 3. Flow of the proposed method.

Step 2 Estimation of pedestrian flow

We used the ratio of the path flow returning to the Mojiko Station to the total amount of observed data to surmise the non-observed flow of people near the event location. The initial value of the ratio was considered as $1/3$ for three return paths; further, this ratio was calculated again from the simulation results. The details are explained in **Section 4.3**.

Step 3 Simulation of pedestrian flow

We used the flow of people estimated in **Step 2** to initialize the simulation. Multi-agent simulations were performed using CrowdWalk [1] (see **Section 5**) with different types of guidance control information, leading to different sets of simulation results.

Step 4 Evaluation of accuracy of simulation results

The accuracy of the simulation results was evaluated by calculating the differences between the observation data and simulation results for the inflow and migration distance. The error evaluation method is explained in **Section 6**. The proportion of people in the next generation of the return path to the Mojiko Station was updated using the most-accurate result.

Step 5 Updating the guidance control information

Using the simulation results from Step 4, a genetic algorithm (GA) operation was performed and the generated individual was renewed (updated) as a new candidate for the guidance control information. The GA operation is explained in **Section 7**.

Step 6 Repeat Steps 2–5

Using the ratio of people using each path updated from Step 4 and the updated guidance control information from Step 5, the simulation process in Steps 2–5 was repeated until the error converged.

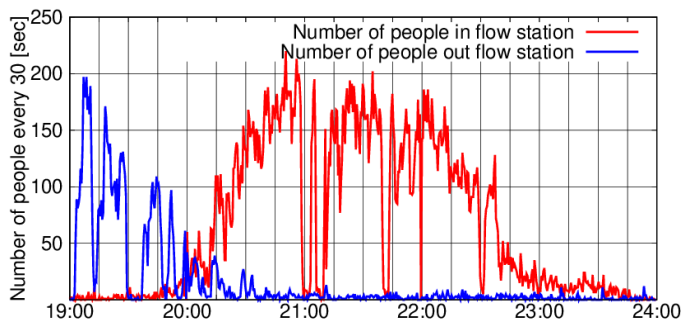


Fig. 4. Inflow (red) and outflow (blue) of users of Mojiko Station measured via RGB-D cameras (2016).

4 Large-scale pedestrian flow measurements

The flow of people can be measured by either measuring the flow of all the people passing through a certain area (e.g., via a video camera or a laser) or measuring all paths taken by a small number of people (e.g., via GPS). To estimate the large-scale flow of people, these two methods are combined to estimate the flow of people in the entire area.

4.1 Pedestrian flow measurement via cameras

In most traffic surveys, pedestrian flow is measured visually. However, this approach is difficult in crowded environments and for long-time measurements. To mitigate these problems, human flow measurements using cameras and lasers are being performed. Recently, low-cost three-dimensional image-acquisition devices, such as stereo cameras and Kinect, have become available. Consequently, research on three-dimensional information processing has progressed rapidly; compared with methods that use only two-dimensional images, the position of pedestrians can be extracted with higher accuracy even in crowded environments [11].

On the event day of the Kanmon Strait Fireworks Display, we installed eight RGB-D cameras near Mojiko Station and performed demonstration experiments to measure the flow in and out of the Mojiko Station. **Figure 4** shows the measurement results. The horizontal axis represents time, and the vertical axis represents the number of people moving every 30 [sec]. The blue line represents the number of people flowing out of the Mojiko Station, and the red line represents the number of people flowing into the Mojiko Station. People began returning to the Mojiko Station at 20:00, immediately after the start of fireworks of the Kanmon Strait Fireworks Display, with the number of people peaking at 20:45. The congestion peak then continued until approximately 22:45, with the inflow

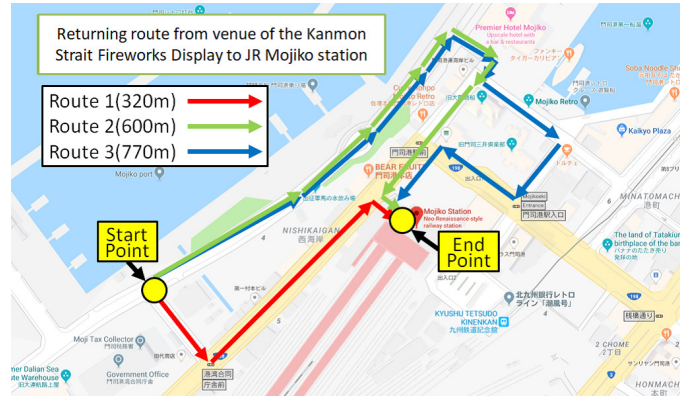


Fig. 5. Three pedestrian flow paths to Mojiko Station.

decreasing thereafter. The number of people flowing into the Mojiko Station is $E(t)$ ($t = 1, \dots, T$).

4.2 Time required to reach Mojiko Station, as measured by GPS

GPS is a system used to determine the position of an object by receiving radio waves sent from satellites. Additionally, the position information obtained by GPS can be used to obtain information about the total travel distance from the departure point to the Mojiko Station and the traveling speed.

After the fireworks of the Kanmon Strait Fireworks Display, pedestrians returning to Mojiko Station from the event location were routed into the three separate return paths, as shown in Fig. 5, which alleviated congestion. 45 subjects equipped with Handy GPS units traveled on each return path from 19:00 to 22:30 after every 15 [min] from the event location to the Mojiko Station, and the trajectory of each path was measured.

Figure 6 shows the measurement results for 2016. The horizontal and vertical axes represent time and the total movement distance of each path to the Mojiko Station, respectively. The pedestrians moved immediately after the fireworks began at approximately 20:00. However, they were caught up in congestion after that time, thereby exceeding the time taken to reach the Mojiko Station by approximately 20 [min]. The congestion relaxed with time, and the flow became smooth again after 22:00. $L^{(n,c)}(t)$ ($t = 1, \dots, T$) is the change in time of the return path for a person walking the c n -th return path.

4.3 Estimation of pedestrian movement

GPS provided the movement trajectory of a specific person who had finished watching the firework, whereas the cameras captured everyone who passed through a specific area. Therefore, by combining these two types of data, the number of

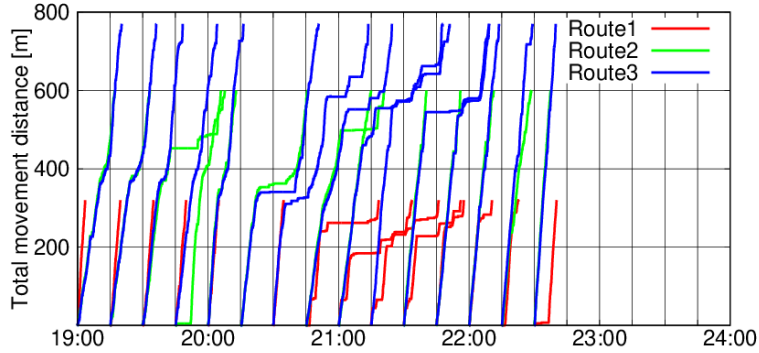


Fig. 6. Pedestrian flows headed to Mojiko Station, as measured by GPS (2016).

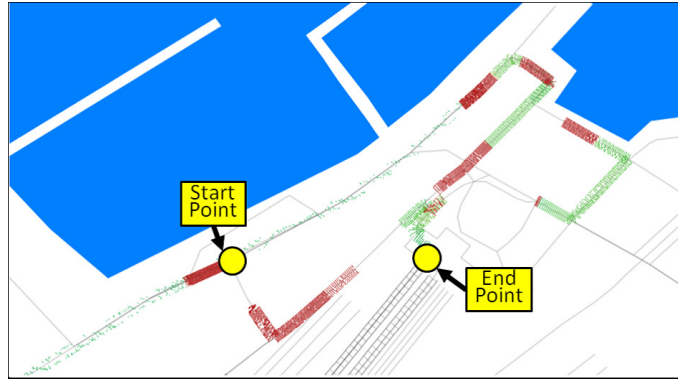


Fig. 7. Simulation after the fireworks of the Kanmon Strait Fireworks Display.

people who started returning from the event location was estimated at each time via a back-calculation:

$$S(t) = \sum_{s=1}^T \sum_{c=1}^3 \begin{cases} E(s) \cdot \mathbf{a}_c(s) & (\text{if } t = s - M(s, c)) \\ 0 & (\text{else}) \end{cases} \quad (1)$$

where c identifies the return path ($c = 1, 2, 3$), $\mathbf{a}_c(t)$ is the ratio of people taking each path, $E(t)$ is the number of people entering Mojiko Station at time t , and $M(t, c)$ is the time required to move from the event location to Mojiko Station on path c . $E(t)$ was measured using the camera, and $M(t, c)$ was measured via GPS. Using **Eq. (1)** and calculating the number of people at the measurement time, we estimate the number $S(t)$ of people departing the event location who were not measured.

5 Estimation of large-scale pedestrian movement via simulation

Measuring the large-scale flow of people in all areas is difficult; therefore, simulation seems effective in such cases. We simulated the crowd flow at the Kanmon Strait Firework Display using the pedestrian simulator CrowdWalk [1]. Because CrowdWalk expresses a move able area with a one-dimensional link and a node, memory consumption is light and a wide range of simulations can be executed at high speed. Moreover, using a social force model [12] to determine the acceleration, pedestrian movement can be calculated precisely and with high reproducibility.

The simulation was initialized with $S(t)$ as the departure state of a person starting to return to the Mojiko Station. In addition, the executive committee controlled the crowd with “stop/advance” signals and “straight-ahead/detour” branches; we represent the guidance control information as \mathbf{x} . If \mathbf{x} and $S(t)$ in **Eq. (1)** are determined, the simulation can estimate the flow of people and $E_s(t)$ and $L_s^{(n,c)}(t)$ can be obtained. We can also estimate $\mathbf{a}_c(t)$ used in **Eq. (1)**.

Figure 7 shows an example of the simulation result for the flow of people after the fireworks of the Kanmon Strait Fireworks Display. In the simulation, the situation people returning to the Mojiko Station during 19:00–24:00 was assimilated into the model. Venue of the Kanmon Strait Fireworks Display and Mojiko Station were set as the measurement start and end points, respectively. The pedestrians branched into each route with a certain probability, where green dots are people moving smoothly and red dots are people caught up in congestion.

6 Evaluating the simulation accuracy

We used the Nash–Sutcliffe model efficiency coefficient (NSE) [13], which is an index for evaluating the accuracy of a model when considering the magnitude of the variance of the data, as an error index for the simulation results. The reproducibility of the model is higher when NSE is closer to unity. NSE evaluates the accuracy of the time T from the start to end of measurement via **Eq. (2)**.

$$NSE(A(t), B(t)) = 1 - \frac{\sum_{s=1}^T (A(s) - B(s))^2}{\sum_{s=1}^T (A(s) - \bar{A})^2} \quad (2)$$

where $A(t)$ is the result obtained experimentally, $B(t)$ is the result obtained by the simulation, and \bar{A} is the overall average of $A(t)$.

Using the number $E(t)$ of people flowing into the Mojiko Station obtained by the camera and the number $E_s(t)$ of people obtained by the simulation, the accuracy was evaluated using **Eq. (3)**.

$$Sim_H = NSE(E(t), E_s(t)) \quad (3)$$

Because the result $E_s(t)$ obtained via simulation assumes orderly behavior, filtering was performed using the cumulative probability in a Gaussian distribution to match the result comprising the actual uncertainty factor.

Furthermore, the accuracy was estimated via **Eq. (4)** using the flow path $L^{(n,c)}(t)$ obtained from the GPS measurements of the three return paths c and the flow path $L_s^{(n,c)}(t)$ obtained by the simulation.

$$Sim_L = \sum_{c=1}^3 \sum_{n=1}^N NSE(L^{(n,c)}(t), L_s^{(n,c)}(t)) \quad (4)$$

We weighted the evaluations of the data measured by camera and GPS which performed an overall accuracy evaluation via **Eq. (5)**.

$$Sim = \alpha \cdot Sim_H + (1 - \alpha) \cdot Sim_L \quad (5)$$

where α is an empirically determined numerical value that adjusts the number of people and the error evaluation values of the flow paths. Herein, the value of α is 0.5.

7 Estimation of guidance control information

Once the situations $S(t)$ of the people returning to the Mojiko Station and the guidance control information \mathbf{x} are determined, $E_s(t)$ and $L_s^{(n,c)}(t)$ can be obtained from the simulation. In particular, $E(t)$ and $L^{(n,c)}(t)$ are measurable; thus, if we can determine the value of \mathbf{x} that is most similar to **Eq. (5)**, we can estimate the flow of people in all areas, including those that cannot be measured. Herein, \mathbf{x} was a set of 0s and 1s expressing “stop/advance” and “straight-ahead/detour” every hour, and it was estimated using a GA.

GA [14] is an optimization method that imitates the genetic and evolutionary mechanisms of living organisms with engineering technology. It prepares solution candidates based on the number of individuals expressed by genes, selects individuals preferentially with high fitness, and searches for solutions while repeating operations such as crossover and mutation. GAs are effective in cases where searching cannot be done conventionally (e.g., by combinatorial explosion) or it is difficult to obtain a solution mathematically or theoretically. However, GAs requires high calculation load and a considerable amount of time compared to other optimization methods. Sometimes, the set parameters do not reach the optimal solution and instead fall into a local optimum. To address the calculation load, we used a parallel-processing distributed GA (DGA) [15], opposition-based learning (OBL) [16], and a two-level orthogonal table.

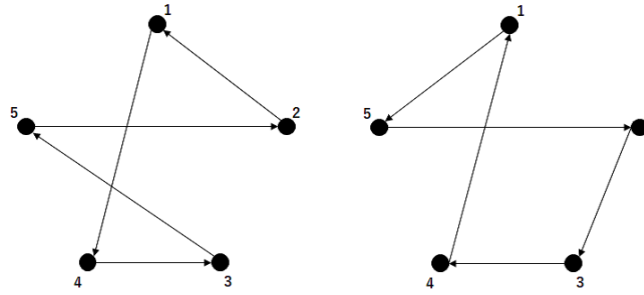


Fig. 8. Migration operation via random ring.

DGA is a parallelized model that divides a population into several groups and manipulates the GA within each island; the operation of DGA selects and exchanges the migrating individuals. Herein, individuals were selected and exchanged via a random ring operator [17] that changed the destination from each island randomly (**Fig. 8**).

OBL is used to speed up the optimization. If $x \in | a, b |$ is a real number, the symmetric point of x is obtained with a center of $| a, b |$ as the mirror image point. This can be expanded to be multidimensional and has the effect of reducing the bias due to the random distribution of initial individuals.

L2048 is the two-level orthogonal table of $2^{2,048}$ design of the Design of Experiments [18]. It is a combination table that can perform multidimensional array experiments of an enormous number of experiments a few times using two types of numbers. It is used for signal control information in of initial individuals in this experiment.

8 Experiment and discussion

Three GA algorithms were evaluated using actual measurement data on the flow of approximately 100,000 people at the Kanmon Strait Fireworks Display measured in 2016.

8.1 Experimental environment

We installed eight RGB-D cameras near Mojiko Station and measured the number $E(t)$ of people entering the Mojiko Station. In addition, individuals with Handy GPS walking three different routes from the start point in **Fig. 7** to the end point after every 15 [min] and total 45 $L^{(n,c)}(t)$ values were measured. We used CrowdWalk [1] to simulate the pedestrian flow. The data from 19:00 to 24:00 were used for measurements and simulation. An example of the simulation results is shown in **Fig. 9**.

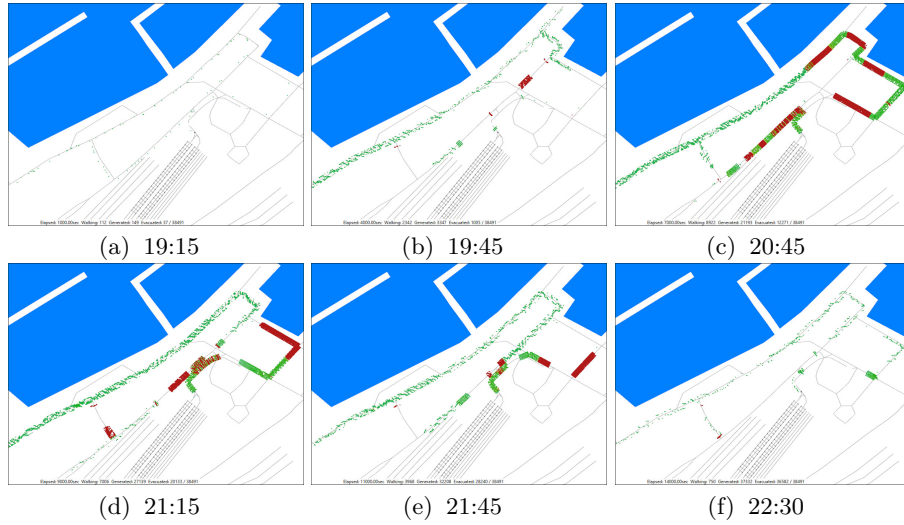


Fig. 9. Pedestrian simulation results after the fireworks of the Kanmon Strait Fireworks Display.

The GA conditions for estimating the parameters are given in **Table 1**. The estimated guidance control information \boldsymbol{x} comprises “stop/advance” control at eight locations and “straight-ahead/detour” control at two locations, i.e., there were controls at total 10 locations. The controls were performed every 1 [min] and the parameters were for total 2,100 dimensions, i.e., 210 [min] \times 10 places from 19:30 to 23:00.

Table 1. Variable list

Parameter	Value
Chromosome Length	2100
Population Size	101
Number of Islands	5
Mutation Rate	1%
Migration Topology	Random Ring
Migration Interval	5
Selection	Tournament
Crossover	Two Point

The number of calculated individuals for each generation was 101 individuals in one island. The generated individuals were narrowed in number via tournament selection, and parameter exchanges of individuals selected by a two-point crossover operation were performed for the next generation. Each island performed an emigration calculation every five generations.

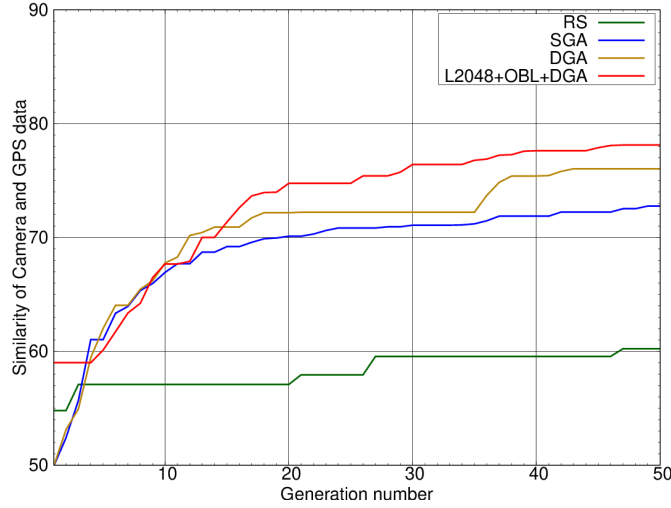


Fig. 10. Similarity of each method.

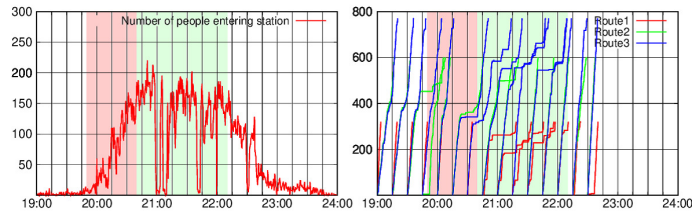
Table 2. The best similarity of each method

Method	Sim	Sim_H	Sim_L
RS	60.2%	69.4%	55.1%
SGA	72.8%	83.7%	61.9%
DGA	76.0%	88.3%	64.8%
L2048+OBL+DGA	78.1%	88.3%	71.2%

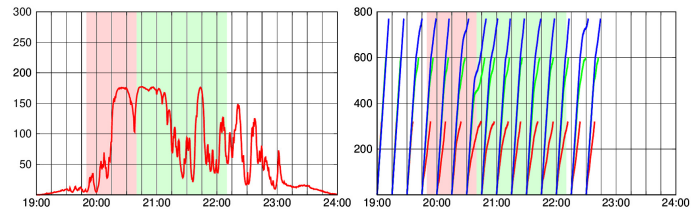
For the computational experiments, we used an Intel CPU Core i7 (4.2 [GHz]) for each island and a computer with 16.0 [GB] of memory (total five computers) to perform migration calculations using random ring [17] operations via the network. The calculation time was approximately 10 [min] per trial, and 20 [h] were required to calculate 101 trials in one generation and perform an accuracy evaluation. Herein, a calculation experiment of approximately 40 days was conducted and the estimation results of 50 generations were evaluated. For comparison, a method was implemented to determine the parameters randomly. To equalize the conditions of the number of calculations, 50 generations were calculated with $101 \times 5 = 505$ trials per generation.

8.2 Experimental results and discussion

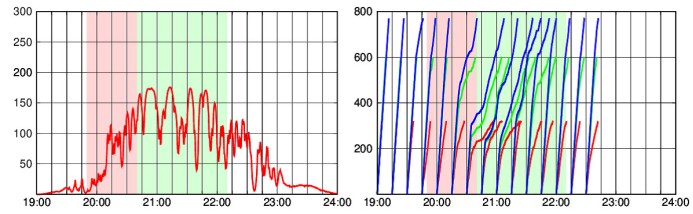
The calculation results are shown in **Fig. 10** and **Table 2**. The horizontal axis represents the generation number, and the vertical axis represents the accuracy of **Eq. (5)**. The red, yellow, and blue lines represent the proposed method, which realizes higher accuracy than the random search represented by the green line.



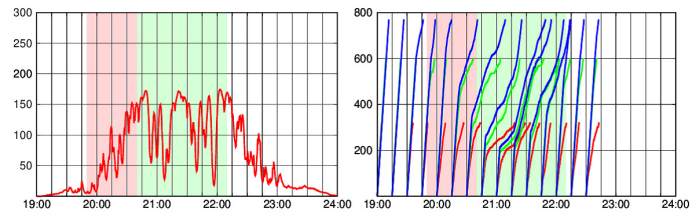
(a) Observation results in 2016



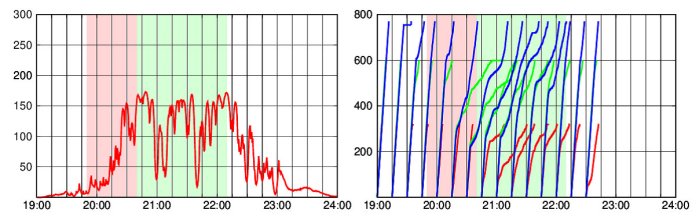
(b) 1st generation



(c) 5th generation



(d) 10th generation



(e) 50th generation

Fig. 11. Observation and simulation results.

Next, we consider each result in **Fig. 11** individually. In **Fig. 11**, the left-hand column shows the number of people measured via the camera and the right-hand column shows the flow paths of the people measured by GPS.

Figure 11(a) shows the results measured in the actual environment, and **Figs. 11(b)–(e)** show the results obtained via simulations. **Figure 11(b)** shows the initial simulation results. By repeating the calculations from **Figs. 11(b)** to **(e)**, the simulation results are clearly close to the actual observation results. In each graph, the time of the fireworks of the Kanmon Strait Fireworks Display is expressed in red and the holding time of this live show is shown in green. The length of the live show was calculated to mitigate congestion after the Kanmon Strait Fireworks Display, and the fireworks display committee members planned to disperse the people returning home immediately after the fireworks display into later time periods.

8.3 Discussion

From **Fig. 10**, the best-proposed method approximated the measurement results with an accuracy of 78.1% using an evolution calculation of 50 generations. With the random search, the same amount of calculations resulted in an accuracy of 60.2%, which shows that our method estimated the parameters effectively. Generally, DA methods are used to deal with large-scale events; therefore, the number of parameters is large and realizing them with high accuracy is difficult. Herein, we dealt with $2^{2,100}$ parameters; however, the proposed method achieved an accuracy of more than 78.1%.

A comparison of **Fig. 11(a)** and **(e)** shows that the inflow of people near the Mojiko Station measured by the camera and the movement of people walking with GPS could be reproduced. In particular, the number of people flowing into the Mojiko Station increased considerably around 21:00 and 21:45, thereby restricting the inflow into the Mojiko Station for a long period of time, which is a situation that the present simulation could also reproduce.

The present simulation provides the trajectories of people entering the Mojiko Station from the venue of Kanmon Strait Fireworks festival and can estimate the flow of people in all areas, including those that cannot be measured directly. For example, **Fig. 12** shows the flow of people near the venue of the Kanmon Strait Fireworks Display where no video camera was installed. Using DA, the number of visitors who move back to the Mojiko Station can be estimated. Usually, it is predicted that many people will start returning home after the end of the fireworks of the Kanmon Strait Fireworks Display; however, from **Fig. 12**, it can be seen that playing the mini live show right after the end of the fireworks resulted in a situation where the returnees were spread out, which reduced the concentration of returnees.

The proposed method can reproduce observation data that are difficult to obtain via camera or GPS using simulation. By reducing the discrete time of the guidance control information from 1 [min] to 30 [s] or to 15 [s], a more realistic result can possibly be obtained. However, with the computers used herein, calculation time of 20 [h] was required for one generation; therefore, calculation

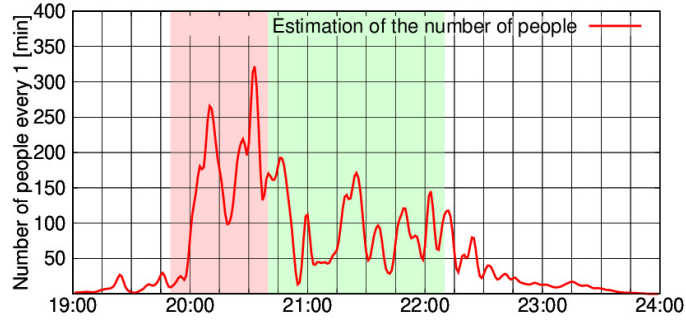


Fig. 12. Estimation of number of people returning from the location of the Kanmon Strait Fireworks Display.

experiments were conducted with 1-min intervals because of the calculation-time restrictions.

9 Conclusions

A method for estimating the flows of people in all areas, including unknown areas, was proposed herein by combining large-scale flow measurement data and performing DA. We confirmed that a parameter space of $2^{2,100}$ can be reproduced with an accuracy of 78.1% by applying the proposed method to the 100,000 human-flow data points measured at the Kanmon Strait Fireworks Display. Moreover, by estimating the state of a person who starts returning from the Kanmon Strait Fireworks Display that could not be measured by the camera, the effect of the event could be determined. To improve the accuracy of the unknown areas in the future, we will increase the number of subjects carrying GPS, reduce the rate of errors between the number of people and distance, and verify the GA operation in other patterns.

10 Acknowledgments

This paper is based on results obtained from a project commissioned by the New Energy and Industrial Technology Development Organization (NEDO). Additionally, we also thank the cooperation of many people, including the Kanmon Strait Fireworks Convention Executive Committee, in acquiring this data.

References

- [1] T. Yamashita, T. Okada, and I. Noda, “Implementation of Simulation Environment for Exhaustive Analysis of Huge-Scale Pedestrian Flow.” *SICE Journal of Control, Measurement, and System Integration*, vol. 6, no. 2, pp. 137–146, 2013.

- [2] E. R. Galea, L. Filippidis, Z. Wang, P. J. Lawrence and J. Ewer, “Evacuation analysis of 1000+ seat Blended Wing Body aircraft configurations: Computer Simulations and Full-Scale Evacuation Experiment.” *Pedestrian and Evacuation Dynamics*, pp. 151–161, 2011.
- [3] E. R. Galea, S. Blake, S. Gwynne and P. Lawrence, “The use of evacuation modelling techniques in the design of very large transport aircraft and blended wing body aircraft.” *The Aeronautical Journal*, vol. 107, no. 1070, pp. 207–218, 2003.
- [4] F. Jia, M. K. Patel, E. R. Galea, A. Grandison and J. Ewer, “CFD Fire Simulation of the Swissair Flight 111 In-flight Fire—Part II: Fire Spread within the Simulated Area.” *The Aeronautical Journal*, vol 110, pp. 303–314, 2006.
- [5] M. Tang and Y. Hu, “Pedestrian Simulation in Transit Stations Using Agent-Based Analysis.” *Urban Rail Transit*, vol. 3, no. 1, pp. 54–60, 2017.
- [6] R. E. Kalman, “A New Approach to Linear Filtering and Prediction Problems.” *Transactions of the ASME Journal of Basic Engineering*, vol. 82, no. 1 pp. 35–45, 1960.
- [7] N. J. Gordon, D. J. Salmond, and A. F. M. Smith, “Novel approach to nonlinear/non-Gaussian Bayesian state estimation.” *Radar and Signal Processing, IEE Proceedings F*, vol. 140, no. 2, pp. 107–113, 1993.
- [8] Y. Sasaki, “Some basic formalisms in numerical variational analysis.” *Monthly Weather Review*, vol. 98, no. 12, pp. 875–883, 1970.
- [9] T. Miyoshi, G. Y. Lien, S. Satoh, “Big Data Assimilation” *Toward Post-Petascale SevereWeather Prediction: An Overview and Progress.* *Proceedings of the IEEE*, vol. 104, no. 11, pp. 2155–2179, 2016.
- [10] S. Motesharrei, J. Rivas, E. Kalnay, “Modeling sustainability: population, inequality, consumption, and bidirectional coupling of the Earth and Human Systems.” *National Science Review*, vol. 3, no. 4 pp. 470–494, 2016.
- [11] M. Onishi, “Analysis and Visualization of Large-Scale Pedestrian Flow in Normal and Disaster Situations.” *ITE Trans. on Media Technology and Applications*, vol. 3, no. 3, pp. 170–183, 2015.
- [12] D. Helbing, I. Farkas, and T. Vicsek, “Simulating dynamical features of escape panic.” *Nature*, vol. 407, pp. 487–490, 2000.
- [13] J. E. Nash, J. V. Sutcliffe, “River flow forecasting through conceptual models Part I - A discussion of principles.” *Journal of Hydrology*, vol. 10, no. 3, pp. 282–290, 1970.
- [14] J. H. Holland, “Adaptation in Natural and Artificial Systems.” *University of Michigan Press/MIT Press*, 1975.
- [15] E. Cantu-Paz, “A survey of parallel genetic algorithms.” *Calculateurs Paralleles, Reseaux et Systems Repartis*, vol. 10, 1998.
- [16] H. R. Tizhoosh, “Opposition-Based Learning: A New Scheme for Machine Intelligence.” In *Proceedings of the International Conference on Computational Intelligence for Modelling Control and Automation (CIMCA-2005)*, Vienna, Austria, pp. 695–701, 2005.
- [17] T. C. Belding, “The Distributed Genetic Algorithm Revisited, *Proceedings of the Sixth International Conference on Genetic Algorithms.* Morgan Kaufmann, San Francisco, CA, pp. 114–121, 1995.
- [18] A. Dean, M. Morris, J. Stufken, and D. Bingham, “Handbook of Design and Analysis of Experiments.” *Chapman and Hall/CRC*, 2015.